

# AFM investigations of self-assembled DOPA–melanin nano-aggregates

Maria Jastrzebska · Iwona Mróz · Bogdan Barwiński · Roman Wrzalik · Stanisław Boryczka

Received: 20 January 2010/Accepted: 28 April 2010/Published online: 11 May 2010  
© Springer Science+Business Media, LLC 2010

**Abstract** The formation of longitudinal, fibril-like structures upon drop drying of the synthetic DOPA–melanin colloidal suspension was investigated. Synthetic DOPA–melanin comprises mainly molecular species derived from the coupling of 5,6-dihydroxyindole and 5,6-dihydroxyindole-2-carboxylic acid monomers that aggregate forming granules. AFM images have shown that for different substrates (mica, glass, gold), melanin granules have a tendency to form aggregates on nanometer-size scale, which in turn self-assemble into fibril-like structures. The deposits are about 250 nm in width and 50 nm in height. The formation of observed deposits has been explained assuming Van der Waals interactions between stacked planar aromatic structures present in melanin protomolecules. These results can support the recent stacked oligomer model for eumelanin protomolecules and provide experimental evidence for formation of organic self-assembled nano-aggregates of melanin polymer.

## Introduction

The importance of molecular self-assembly in biomolecular systems has invigorated the field of structural investigations and the results of significant research efforts provided new insights into molecular interactions and were utilized in areas ranging from molecular electronics to tissue engineering and material science [1–4].

Recently, the self-assembly of many macromolecules has been reported, for example, self-assembly of amyloid-like fibrils into stable, conductively and intrinsically fluorescent biomolecular nanowires [5, 6] or formation of liquid crystalline pattern of DNA upon droplet drying [7].

In the present paper, we report the formation of longitudinal, fibril-like structures built from nano-aggregates of planar melanin oligomers.

Melanin pigments are found in many organisms and belong to the class of polycyclic biopolymers with physical and chemical properties very attractive for the materials science. For instance, melanins are known as photoprotective agents transforming the adsorbed photon energy to heat. Meng and Kaxiras [8] have found that this energy conversion takes place in a remarkable short timescale of about 100 fs. For solid, powdered synthetic DOPA–melanin the charge hopping process was postulated to be the main mechanism involved in the dielectric response of the melanin polymer [9]. Synthetic DOPA–melanin shows also photoconductivity [10] and the persistent electron spin resonance (ESR) signal [11, 12]. Melanin biopolymers have also been proposed for optoelectronic and photovoltaic applications [13, 14].

The molecular structure and physical properties of melanin have been intensively investigated [11, 15–20], however, the detailed knowledge of its structure, especially at the molecular level, is still not well documented.

M. Jastrzebska (✉)  
Department of Radioisotope Diagnostics and  
Radiopharmaceuticals, Faculty of Pharmacy, Medical University  
of Silesia, 41-200 Sosnowiec, Poland  
e-mail: maja@sum.edu.pl

I. Mróz · B. Barwiński  
Institute of Experimental Physics, University of Wrocław,  
50-204 Wrocław, Poland

R. Wrzalik  
Department of Biophysics and Molecular Physics, Institute  
of Physics, University of Silesia, 40-007 Katowice, Poland

S. Boryczka  
Department of Organic Chemistry, Faculty of Pharmacy,  
Medical University of Silesia, 41-200 Sosnowiec, Poland

The lack of unquestionable description of the melanin structure is a factor contributing greatly to the uncertainties related to its biological functions.

Synthetic DOPA-melanin can be obtained by oxidation of 3,4-dihydroxyphenylalanine (DOPA) and is known as a polymer modelling natural eumelanins. Eumelanin is a brown-black pigment derived from tyrosine following its conversion to dihydroxyphenylalanine. It is generally accepted that eumelanin as well as synthetic DOPA-melanin consist mainly of 5,6-dihydroxyindole (DHI) and 5,6-dihydroxyindole-2-carboxylic acid (DHICA) monomer units, shown in Fig. 1. These monomers can be in various oxidation states and are thought to be linked randomly with each other and some precursor molecules to form oligomers. Recently, structural models of eumelanin protomolecules have been examined to account for the observed melanin properties and structure–activity relationship. Two qualitatively different models, the cross-linked heteropolymer model and the stacked oligomer model have been argued [20, 21]. However, there is more evidence in support of planar stacking in melanin protomolecules. Meng and Kaxiras [20] described the ‘stacked oligomer’ model containing an interior porphyrin ring. This stacked protomolecule model appeared to agree with the X-ray diffraction experiments performed by Cheng et al. [22, 23]. Many theoretical and experimental studies have been performed in order to examine the stacked oligomer model for eumelanin [19, 20, 24–26]. More recently, Abbas et al. [15] described formation of melanin film using spray deposition and suggested possible charge transport mechanism by means of delocalized  $\pi$  states along the stacked planar secondary structure of melanin protomolecule.

Formation of self-assembled molecular structures is dominated by two interactions, those between the substrate and adsorbate and those between the adsorbates themselves. In this paper, these two interactions and the mechanism of the droplet drying process are argued in the course of analyzing DOPA-melanin self-assembled structures.

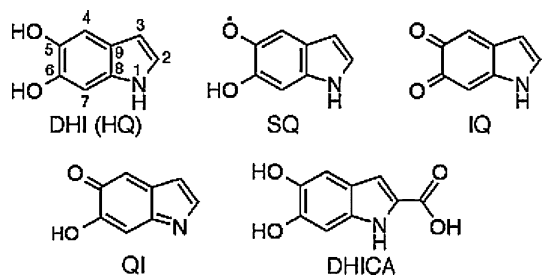


**Fig. 1** Monomer components of eumelanin [11]. Hydroquinone (DHI), 5,6-dihydroxyindole-2-carboxylic acid (DHICA) and their redox forms

## Materials and methods

### Preparation of the samples

Melanin was synthesized using a previously reported procedure [9–11]. Briefly, aqueous solution of L-DOPA (3,4-dihydroxy-L-phenylalanine; Sigma-Aldrich (St.Louis, MO, USA)) in double distilled water (0.005 mol/l) was aerated at 20 °C for 72 h. After that time, the solution became dark-brown and slightly basic (pH = 8.5). However, the final acidification was omitted because the basic pH allows maintaining pigments in the colloidal form without precipitation of melanin granules. Moreover, low pH promotes the aggregate growth and sedimentation while high pH induces breaking up of the granules to small particles with lower degree of polymerization [27].

In experiments, three different solid substrates were used, i.e., glass microscope slides (thickness 1 mm, Fisher-finest Premium, Fisher Scientific, Pittsburg, PA, USA), freshly cleaved muscovite mica (SPI Supplies® Mica Sheets, Strips and Discs) and a gold film.

A microscopic glass slide was pretreated with chromic acid, rinsed with purified water and dried for 6 h at 25 °C before use. Next, a droplet of about 40  $\mu$ L of the solution, was deposited onto a microscopic glass slide with a syringe (Hamilton, Reno, NV, USA). The droplet was spread over the solid surface until the equilibrium was established between the capillary and hydrostatic pressures. Then, the droplet was left for evaporation at room temperature. Over time, the liquid evaporated leaving dark-brown deposit, mainly at the edge of the evaporating fluid. This edge-deposited material was next subjected to further investigations.

The gold film was deposited by vacuum evaporation onto the freshly cleaved mica substrate at room temperature. The mass thickness of the film was estimated from the geometry of the evaporation system as equal to 50 nm.

### AFM measurements

The AFM imaging was performed using the NanoScope E (Digital Instruments, Santa Barbara, California, USA) working in the contact mode. The microscope was equipped with the standard NP-S probe (NanoProbe™, Veeco, Plainview, NY, USA). The nominal spring constant of the V-shaped cantilever used was 0.32 N/m. The applied constant force was about 20 nN. We used AS-12"E" scanner therefore the maximum size of images in both  $X$  and  $Y$  horizontal directions was 13  $\mu$ m. The maximum height (Z-limit) was 3.8  $\mu$ m. Height and deflection signals were recorded simultaneously. The images were obtained with lateral and height resolutions of about 10 nm and 1 nm, respectively. The images were processed with the software package WSxM [28].

## Results and discussion

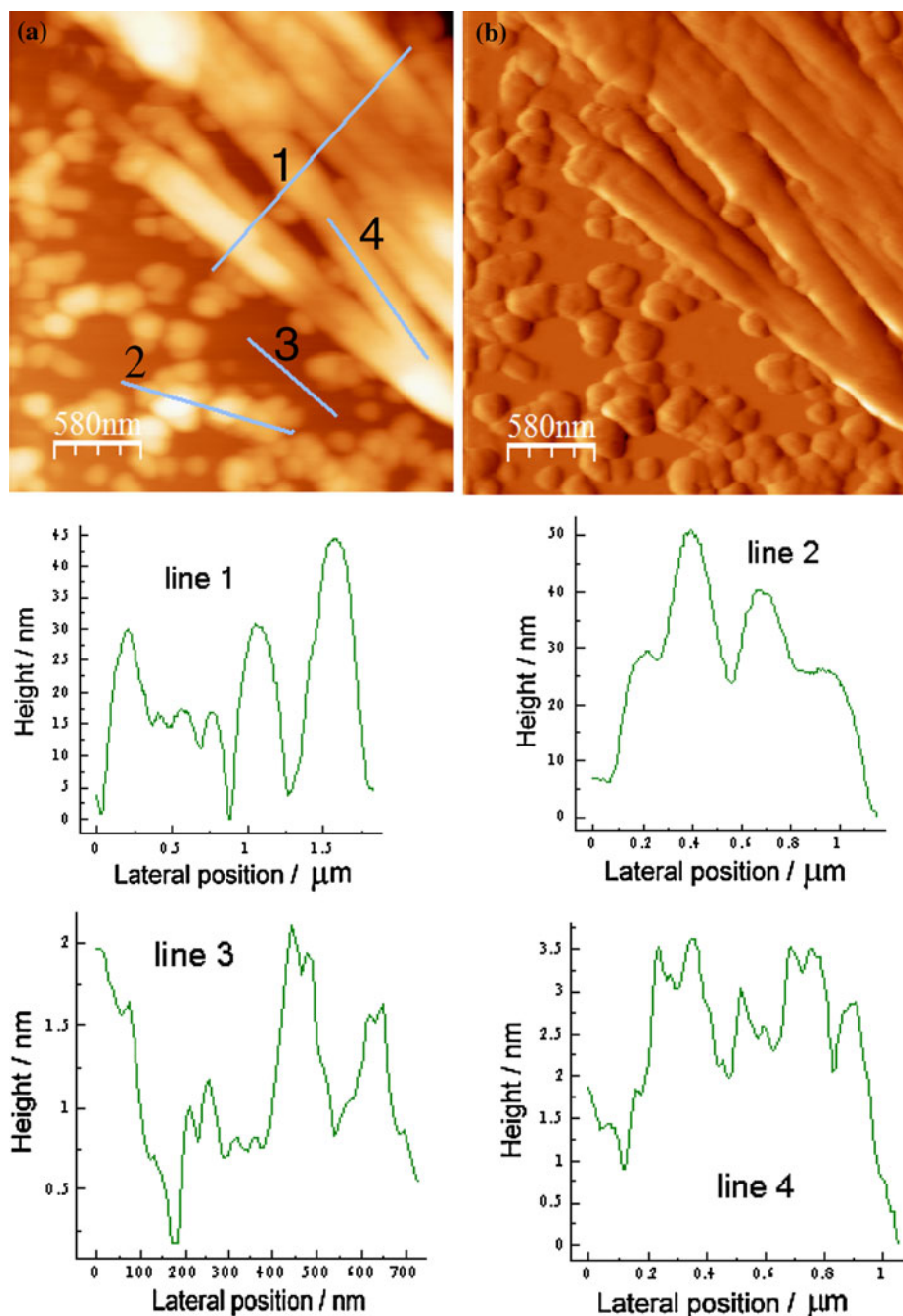
Models of single droplet drying suggest that the rate of evaporation is faster at the edge of the droplet, therefore, colloidal particles accumulate and compact along the edge, forming a solid deposit on the flat substrate. However, the formation of the deposit is also influenced by the substrate–adsorbate interactions.

In our experiment, the surface of gold substrate exhibited typical hydrophobic properties. Therefore, an aqueous colloidal droplet formed spherical segment on its surface.

Electrochemical studies confirmed the hydrophobic character of gold, however, wetting of gold by water may be observed, e.g., shortly after quenching or etching the outer gold layer [29]. The properties of gold surfaces used for AFM sample preparations are described in detail in [30, 31].

Glass is known as a hydrophilic material because water contact angle with its surface is usually in the range from 20° to 40°. However, even more hydrophilic character can be observed for mica substrates. On mica, an aqueous droplet spreads easily over the surface. Further, freshly

**Fig. 2** AFM images of the DOPA–melanin deposits on mica. **a** Height, **b** deflection. The profiles are taken along the lines marked on the height image. The average width and height of the stick-like structures are  $250 \pm 30$  nm and  $30 \pm 10$  nm, respectively. For granule objects, the transverse and height dimensions are  $200 \pm 30$  nm and  $30 \pm 15$  nm, respectively



cleaved, unmodified mica is hydrophilic and negatively charged due to silanol groups ( $\text{Si}-\text{OH}$ ) exposed on the surface [32] that may be involved in formation of hydrogen bonds and sorption of cations on the mica surface. Hydrophilic properties of muscovite mica and glass surfaces are described in [33, 34]. Erikson et al. [34] found that muscovite mica was more negatively charged than glass and this affected the adsorption of surfactants and proteins.

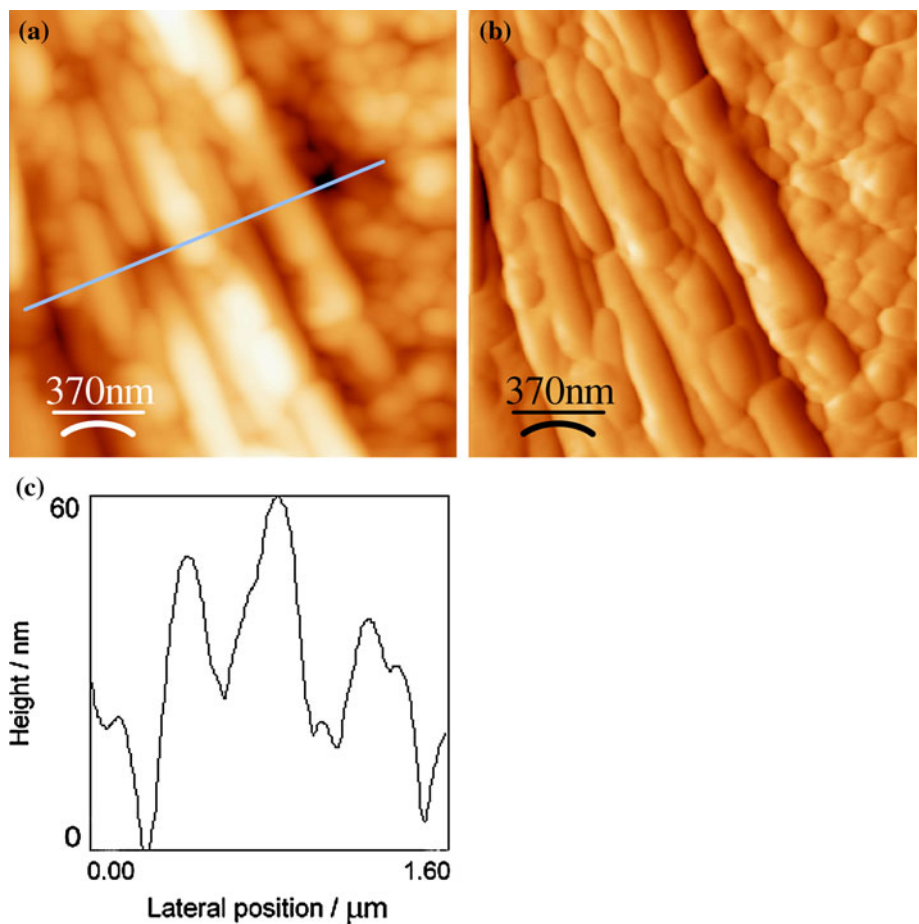
It has been found that for all three substrates used, the deposits showed strong anchoring near the three-phase line. AFM imaging has been performed in the central region of the deposited peripheral ring. It should be noted that the observed deposits have been formed from the structures in the suspension state, where most colloidal particles are suspended in the bulk.

Figure 2 shows the height and deflection AFM images of the longitudinal, stick-like structures formed on the mica substrate. It can be observed that they run approximately parallel and are well separated from each other, while in the lower left part of these images the DOPA–melanin colloidal granules are seen. Figure 2 shows also profiles taken along the following lines: 1—across the deposits giving their dimensions, i.e., width and height over the

substrate surface; 2—across the colloidal granules showing their dimensions; 3—topography of the mica substrate surface; and 4—surface topography of the individual stick-like structure. The average width calculated as a half-width of the peak and the average height of the deposits are equal to  $250 \pm 30$  nm and  $30 \pm 10$  nm, respectively. For granules, the average transverse and height dimensions are equal to  $200 \pm 30$  nm and  $30 \pm 15$  nm, respectively, and are in the ranges found for natural melanin pigments. For example, the eumelanin from the ink sack of *Sepia officinalis*, the dimensions of spherical granules were found in the range of 100–200 nm [35, 36]. Furthermore, it is noticeable that granules and the stick-like structures have similar dimensions giving rise to supposition that granules can serve as building-block units to construct longitudinal structures. In addition, it can be concluded that the building-blocks are tightly packed inside the deposit as no significant gaps between the blocks are observed and the profiles taken along the flat substrate and the deposit (Fig. 2, lines 3 and 4) are similar. The small differences in the height that are seen for both profiles occur as a result of the image recording.

Figure 3 shows AFM images of the deposits obtained on the glass surface. It is well seen that longitudinal structures

**Fig. 3** AFM images of DOPA–melanin deposits on the glass substrate. **a** Height, **b** deflection, **c** profile taken along the line seen in height image. The width and height of the longitudinal deposits are  $250 \pm 30$  nm and  $50 \pm 20$  nm, respectively



are composed of colloidal granules. Consequently, the width and height of the stick-like structures are equal to  $250 \pm 30$  nm and  $50 \pm 20$  nm, respectively.

In Fig. 4 the surface topography of the gold substrate is shown. The average dimensions of gold grains along X- and Z-axes are equal to  $40 \pm 10$  nm and  $6 \pm 3$  nm, respectively.

The stick-like structures have been also self-assembled on the gold substrate, they are seen in Fig. 5. The profile taken across the deposits shows the dimensions of some individual longitudinal structures, which are  $200 \pm 50$  nm and  $35 \pm 10$  nm along X- and Z-axes, respectively. In comparison to the hydrophilic substrates, the deposits on gold show smaller dimensions along both X- and Z-axes.

The AFM images have shown that for different substrates with varying hydrophilicity melanin granules have a tendency to be joined after drop drying and form the variable-sized aggregates, which in turn self-assembled into stick-like structures. Two main phenomena can influence this self-assembly process, first—particle flow dynamics at the edge of the drop upon drying and the second—interaction between DOPA–melanin aggregates. It has been argued [37, 38] that the main cause for particle self-assembly into array structures is the capillary force generated by the menisci formed around the particles during

the drop drying. According to [37], the menisci formed around two granules trapped in the wedge region will generate two types of immersion forces: normal and lateral. The lateral force tends to attract and bring granules together while the normal force tends to adhere granules to the substrate. Interactions between nano-granules themselves are responsible for the longitudinal arrangement and formation of stick-like structures. According to the recent models of the eumelanin macromolecules, we assume that the interactions between granules result mainly from the stacked structure of the melanin protomolecules. Eumelanin protomolecules consist of the Van der Waals interacting stacks of the planar aromatic structures built from monomer units, i.e., hydroquinone, indolequinone and its tautomers including quinone-methide and quinone-imine (Fig. 1). There is an extensive  $\pi$ -delocalization within the individual oligomeric sheet. Recently, it has been also proposed that such monomer units can form a tetramer planar unit in an arrangement that contains an interior porphyrin ring [20]. It was argued that besides Van der Waals interactions, the additional covalent bonds between two neighbouring tetramers can be formed when they are stacked. Consistently with the model, the interlayer covalent bond formation makes the melanin protomolecules more stable and could be responsible for the insolubility of

**Fig. 4** AFM surface topography of the gold substrate. **a** Height, **b** deflection, **c** height profile taken along the marked line. X- and Z-axes dimensions of the gold grains are  $40 \pm 10$  nm and  $6 \pm 3$  nm, respectively

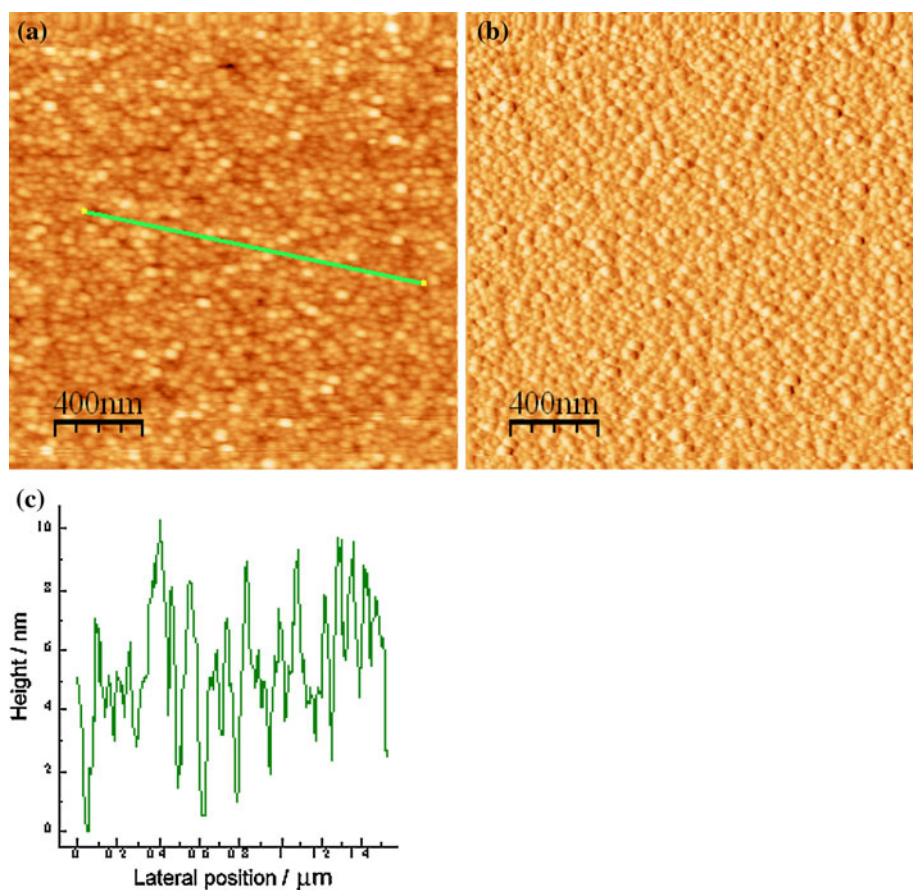
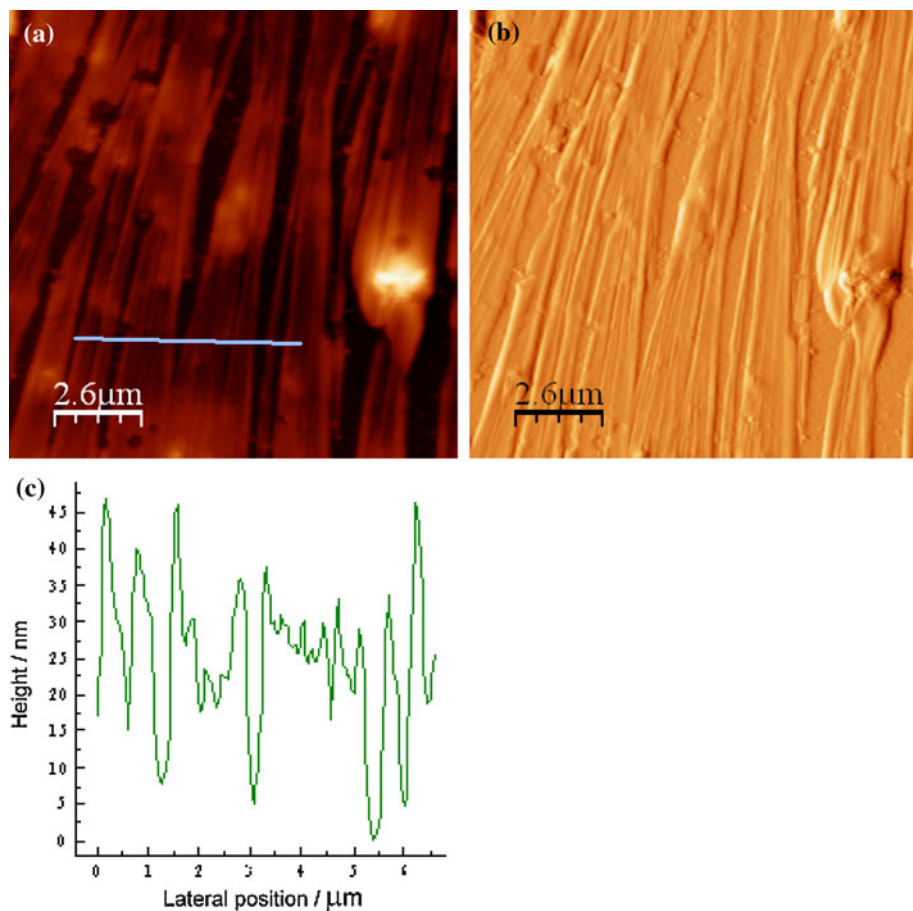


**Fig. 5** AFM images of the DOPA–melanin deposits on the gold substrate. **a** Height, **b** deflection, **c** height profile taken along the marked line. X- and Z-axes dimensions of the longitudinal structures are  $200 \pm 50$  nm and  $35 \pm 10$  nm, respectively



melanin. It seems that the Van der Waals stacking is mainly involved in longitudinal arrangement of nano-granules.

In conclusions, the presented results appeared to support a recently proposed stacked oligomer model for eumelanin protomolecules. Self-assembly of melanin nano-aggregates is governed mainly by interactions between granules themselves. Interactions of the colloidal suspension with the substrate influences the shape of a droplet and hence the drying process. However, it has been observed that for the mica substrate more numerous and better separated deposits were formed in comparison to glass and gold substrates.

Further studies are needed to explore possible charge transport along the deposited structures.

**Acknowledgements** This work was partially supported by the Grant No. KNW-1-040/09. The authors are grateful to Professor A. Ciszewski from the Institute of Experimental Physics, University of Wroclaw, Poland, for his scientific guidance.

## References

- Worrall JAR, Górná M, Pei XY, Spring DR, Nicholson RL, Luisi BF (2007) Biochem Soc Trans 35(3):502
- Duggal R, Hussain F, Pasquali M (2006) Adv Mater 18:29
- Briseno AL, Mannsfeld SCB, Jenekhe SA, Zhenan Bao, Xia Y (2008) Mater Today 11(4):38
- Akutagawa T, Ohta T, Hasegawa T, Nakamura T, Christensen CA (2002) Proc Natl Acad Sci USA 99(8):5028
- del Mercato LL, Pompa PP, Maruccio G, Tore AD, Sabella S, Tamburro AM, Cingolani R, Rinaldi R (2007) Proc Natl Acad Sci USA 104(46):18019
- Scheibel T, Parthasarathy R, Sawicki G, Lin X-M, Jaeger H, Lindquist SL (2003) Proc Natl Acad Sci USA 100(8):4527
- Smalyukh II, Zribi OV, Butler JC, Lavrentovich OD, Wong GCL (2006) Phys Rev Lett 96:177801(4)
- Meng S, Kaxiras E (2008) Biophys J 95:4396
- Jastrzebska M, Kocot A, Vij JK, Zalewska-Rejdak J, Witecki T (2002) J Mol Struct 606:205
- Jastrzebska M, Kocot A, Tajber L (2002) J Photochem Photobiol B 66:201
- Meredith P, Sarna T (2006) Pigments Cell Res 19:572
- Sarna T, Plonka PM (2005) In: Eaton SS, Eaton GR, Berliner LJ (eds) Biomedical EPR—Part A free radicals, metals, medicine and physiology, biological magnetic resonance, vol 23. Kluwer Academic/Plenum Publishers, New York
- Diaz P, Gimeno Y, Carro P, Gonzalez S, Schilardi PL, Benitez G, Salvarezza RC, Creus AH (2005) Langmuir 21:5924
- Subianto S, Will G, Meredith P (2004) International Patents Application PCT/AU20047001244
- Abbas M, Amico FD, Morresi L, Pinto N, Ficcadenti M, Natali R, Ottaviano L, Passacantando M, Cuccioloni M, Angeletti M, Gunnella R (2009) Eur Phys J E 28:285

16. Zajac GW, Gallas JM, Cheng J, Eisner M, Moss SC, Alvarado-Swaigood AE (1994) *Biochim Biophys Acta* 1199(3):271
17. Liu Y, Simon JD (2003) *Pigment Cell Res* 16:606
18. Tran ML, Powell BJ, Meredith P (2006) *Biophys J* 90:743
19. Kaxiras E, Tsolakidis A, Zonios G, Meng S (2006) *Phys Rev Lett* 97:218102(4)
20. Meng S, Kaxiras E (2008) *Biophys J* 94:2095
21. Littrell KC, Gallas JM, Zajac GW, Thiagarajan P (2003) *Photochem Photobiol* 72(2):115
22. Cheng J, Moss SC, Eisner M, Zschack P (1994) *Pigments Cell Res* 7:255
23. Cheng J, Moss SC, Eisner M (1994) *Pigments Cell Res* 7:263
24. Stark KB, Gallas JM, Zajac GW, Eisner M, Golab JT (2003) *J Phys Chem B* 107:11558
25. Stark KB, Gallas JM, Zajac GW, Golab JT, Gidanian S, McIntire T, Farmer PJ (2005) *J Phys Chem B* 109:1970
26. d'Ischia M, Crescenzi O, Pezzella A, Arzillo M, Panzella L, Napolitano A, Barone V (2008) *Photochem Photobiol* 84:600
27. Crippa PR, Horak V, Prota G, Svoronos P, Wolfram L (1989) In: *The alkaloids*. Academic Press Inc., New York
28. Horcas I, Fernandez R, Gomez-Rodriguez JM, Colchero J, Gomez-Herrero J, Baro AM (2007) *Rev Sci Instrum* 78:013705
29. Cognard J (1984) *Gold Bull* 17(4):131
30. Amrein M, Müller DJ (1999) *Nanobiology* 4:229
31. Smith T (1980) *J Colloid Interface Sci* 75:51
32. Maslova MW, Gerasimowa LG, Forsling W (2004) *Colloid J* 66(3):322
33. Kindt JH, Sitko JC, Pietrasanta LI, Oroudjev E, Becker W, Viani MB, Hansma HG (2002) *Methods Cell Biol* 68:213
34. Erikson C, Blomberg E, Claesson P, Nygren H (1997) *Colloids Surf B* 9:67
35. Liu Y, Simon JD (2003) *Pigments Cell Res* 16:72
36. Clancy CMR, Nofsinger JB, Hanks RK, Simon JD (2000) *J Phys Chem B* 104:7871
37. Nikolov AD, Wasan DT (2009) *Ind Eng Chem Res* 48(5):2320
38. Parisse F, Allain C (1997) *Langmuir* 13(14):3598